EXPERIMENTS ON BARYON NUMBER NON-CONSERVATION

M.KOSHIBA

ICEPP* and Department of Physics,
Faculty of Science, University of Tokyo

1. INTRODUCTION

Perhaps one should begin with the historical survey of the subject. However, there recently appeared two, one theoretical[1] and one experimental[2], excellent reviews. Hence, I shall restrict myself to the motivations why we are seriously working on proton decay experiment.

Despite the great successes of the standard Electroweak Theory, there are still a number of long unanswered questions. Why does the electric charge of a proton so exactly cancell that of an electron? Why does the matter dominate over the anti-matter in the Universe? Why do we have the repetitions of fundamental fermion families;(u,d,ν_e,e), (c,s,ν_μ,μ), and (t,b,ν_τ,τ)? What determines the fundamental fermion mass spectrum? Why do the two coupling constants in the electroweak theory have the relation as specified by the experimentally determined Weinberg-Salam angle?

Putting these questions aside for a moment, we consider a conceivable decay process, $(\text{proton} \rightarrow e^+ + \gamma)$. This process has never been observed experimentally, while it can satisfy the energy-momentum conservation, the angular momentum conservation, and the electric charge conservation. We were taught in school that there are the additional conservation laws of baryon number and of lepton number which are not satisfied in this decay process. If there is such an exact conservation laws as the electric charge conservation, there has to be a long range force, like Coulomb force, the source of which is the baryon number. Experimental searches for such an long range force, however, set the upper limit of its strength at 10^{-9} of the gravitational force.

In 1973 Pati and Salam[3], and in 1974 Georgi and Glashow[4] published the theories which attempted the unification, in the form of a local gauge field theory, of the three forces, strong, weak, and electromagnetic. These are the first two versions of what we now call the grand unified theories, GUTS. These theories not only answer some of the questions I mentioned above, but also predict the proton decays violating the baryon number as well as the lepton number conservations. The Georgi-Glashow theory took SU(5) as the underlying symmetry group, which is the smallest simple group containing SU(3) for strong interaction, SU(2) for weak interaction, and U(1) for electromagnetic interaction. It predicted the proton life time in the range of 10^{30} years and the decay$(p \rightarrow e^+\pi^\circ)$ as the dominant decay mode. This triggered the serious attempts on the part of experimentalists for detecting proton decay. A hundred ton of material, containing 6×10^{31} nucleons, will then produce 60 nucleon decays per year for 100% detection efficiency. Such a low rate for the size of detector forces the experiment to be done deep underground in order to avoid the cosmic ray background.

The effects of cosmic ray muons are indeed greatly reduced in the underground sites, but we shall see that the neutrino, resulting from the decays in the atmosphere of the cosmic ray produced pions and/or kaons, is still the major obstacle against the definite experimental proof of proton decay.

2. ON-GOING PROTON DECAY EXPERIMENTS

The on-going proton decay experiments can be devided into two categories, the tracking calorimeter type and the Water Čerenkov type.

* International Center for Elementary Particle Physics

When a mass of water is surrounded by sufficient photosensitive area, say $\gtrsim$ 20% of the entire surface, one can distinctively recognize the individual Čerenkov rings of the secondary particles. We shall call this type of detector "Imaging Water Čerenkov" detector, hereafter refered to as IWC. An existing example of this kind is KAMIOKANDE[5].

The latest version of calorimeter type detector, e.g., Frejus[6] experiment, has the fine granularity of 0.5cm x 0.5cm cross-section counters. We shall refer to this type of detector as "Fine Grain Tracking calorimeter", abreviated as FGTC.

Table 1. Comparison of Imaging Water Čerenkov and Tracking Calorimeter for proton decay

	Imaging Water Čerenkov (photocathode coverage $\gtrsim$20%)	Tracking Calorimeter
Material to look at	H_2O. homogeneous, (11% free P)isotropic.	Fe; inhomogeneous, anisotropic.
Nuclear Effects	None in H. Substantial in O.	Worse in Fe than in O.
$\|\Delta r\|$	~50cm at present, $\lesssim$10cm in sight.	0.5 ~ 5cm at present.
Direction of motion	No ambiguity whatsoever.	Possible in favorable cases.
Means of detection	Č-light of charged particle of $\beta>0.75$.	Ionization of charged particle in gas counter.
Threshold	$\gtrsim$10 MeV $e^{\pm},\gamma$, $\gtrsim$200 MeV $\mu^{\pm}$	$\gtrsim$16 MeV $e^{\pm},\gamma$, $\gtrsim$190 MeV $\mu^{\pm}$
Separation $e^{\pm}\gamma/\mu,\ \pi$	Good	Fair
Separation $e^{\pm}/\gamma$	Probably yes(for 40% coverage and timing).	Maybe in some cases.
Separation $\mu^{\pm}/\pi^{\pm}$	Probably yes(for 40% coverage and timing).	Maybe in some cases.
dE/E for shower	~ $3\%/\sqrt{E(GeV)}$	~ $20\%/\sqrt{E(GeV)}$
μ-e decay detection	$\mu^{\pm} \to e^{\pm}$ ~70% at present. $\gtrsim$90% in sight.	$\mu^{+} \to e^{+}$ ~ 35%
Polarization of $\mu^{\pm}$	Yes.	Difficult
Cost/(M$)	3 Kton(20% coverage)/1.5 32 Kton(40% coverage)/15	1 Kton(0.5cm x 0.5cm counter) /~ 7
Future outlook	Observation of Solar B[8] ν_e's by ν_e-e elastic scattering probably possible. $\gtrsim$10 Kton detector forseeable.	Multi K ton detector not forseeable. No possibility for ν-astronomy.

In Table 1, a comparison is made of the performances of the two types of detector for nucleon decay experiment.

In IWC the material to look for nucleon decays is water which contains 11% free proton. There is the hope of observing free proton decay without the obscuring nuclear secondary effects which we shall see is the main cause of the ambiguity in analysing the data. The homogeneity and the isotropy of water would be of great advantage in making the accelerator ν beam test.

The use of Fe sheets in FGTC makes it inhomogeneous and anisotropic. In the case of NUSEX[7], a FGTC, the ν-beam tests were given at 0° and 45° to the Fe plane normal but not at glancing angles to the Fe plates. We have to expect more nuclear effects in Fe nucleus than in O nucleus.

The vertex determination is certainly much better in FGTC than in IWC, as shown in the third row of Table 1.

In IWC there is no ambiguity whatsoever as regards to the direction of motion of a particle, while in FGTC one can infer the direction of motion only in some favorable cases, e.g. the increase of multiple scattering on long tracks and/or the measurement of dE/dx along the well defined tracks.

It is usually said that the tracking calorimeter can observe low energy particles which the water Čerenkov detector can not get any signal. However, the particle detection thresholds are almost the same for the two types of the detector as can be seen in the sixth row.

The separation of showering particles, e, γ and π^0, from non-showering particles, μ and π, can be made almost equally well in both IWC and FGTC.

The separation of the e-initiated shower from the γ-initiated shower is obviously more difficult and has not been achieved in any existing detectors. However, the time resolved amplitude analysis of IWC, with $\gtrsim$ 40% photocathode coverage, gives a reasonable hope of achieving this goal by looking at the early stage of cascade development, i.e., by eliminating the slightly delayed diffuse light near the outer boundary of the initial Čerenkov cone.

The separation of μ from π is still more difficult, because for the same Č cone opening, i.e. for the same velocity, the difference in the photoelectron number is only 30%. Here again, the next generation IWC of 40% photocathode coverage renders a reasonable hope of making this separation.

The energy resolution of shower energy is definitely better in IWC. In IWC the total track length of the shower is directly measured, while in FGTC it is the sampling at some intervals with the detector of finite size larger than the average inter particle distance of a shower.

The detection probability of $\mu \to e$ decay signal is much better in IWC, 70% at present and $\gtrsim$ 90% forseeable in the next generation IWC, while in FGTC only $\mu^+ \to e^+$ decays are observable. μ^-s are absorbed in Fe nucleus while in O nucleus they decay rather than get absorbed.

Interesting possibility in the case of IWC is its capability of measuring the polarization of decaying μ's from the observation of the angular distribution of e's. This is possible due to the uniform detection efficiency and to the less multiple scattering of the decay e's in IWC. This information will be valuable in restricting the models of proton decay, if they decay at all.

The cost is cheaper for IWC, proportional to the surface, than for FGTC, proportional to the volume, and this tendency becomes more pronounced as the detector gets bigger and bigger.

The last, and not in the least unimportant, remark about the comparison of the two detector types is the fact that the IWC offers the unique possibility of observing Solar B^8 ν's, $\lesssim$ 14 MeV, by means of the $\nu_e - e^-$ elastic scattering in which the direction and the energy spectrum of the incident ν's are well reflected in those of the scattered electrons. This possibility will be discussed again later in this text.

The on-going proton-decay experiments are summarized in Table 2-a, tracking calorimeters, and in Table 2-b, water Čerenkov detectors.

The first column gives the name of the experiment, the geomagnetic latitude, and the depth underground in meter water equivalent of the experimental site. In the second column are given the total mass, the fiducial mass, the year of operation and the data analysed as of July 1984. In the third column the thresholds for particle recognition are shown. In the last column are given the remarks pertinent to the experiment.

We shall now look at the individual experiments.

Kolar Gold Field, K.G.F.[8], experiment is the earliest dedicated experiment on proton decay. The India-Japan collaboration began data taking in late 1980 and claimed the observation of a number of candidate events. Fig.1 shows their two candidate events together with the structure of the detector. It is the alternate layers of X-counters and Y-counters with 1.2cm thick Fe plates in between.

The counters are 10cm x 10cm in cross-section of 0.23cm Fe wall thickness and are

Table 2-a Calorimeter Experiments

Experiment Geomag.Lat. Depth	Total mass Fid. mass Year of op. Data as of July '84	Particle recognition	Remarks
K.G.F. 3°N 7000m.w.e.	140 ton Fe 60 ton Fe 1980 ~ 180 ton-yrs.	$\gtrsim$250 MeV $\pi^{\pm}$ $\gtrsim$210 MeV $\mu^{\pm}$ $\gtrsim$100 MeVγ,$e^{\pm}$	1.2cm thick Fe. 10cmx10cm proportional counters of 0.23cm Fe wall. dE/dx measurable. Early start. Size, 6mx4mx4m.
NUSEX 50°N 5000m.w.e.	150 ton Fe 100 ton Fe 1982 ~ 220ton-yrs.	$\gtrsim$230 MeV $\pi^{\pm}$ $\gtrsim$200 MeV $\mu^{\pm}$ $\gtrsim$50 MeVγ,$e^{\pm}$	1.0cm thick Fe. 1cmx1cm resistive streamer tubes. X-Y read-out on the same tube plane. ν-beam test given. Size, 3.5mx3.5mx3.5m.
Frejus 50°N 4400m.w.e.	800 ton Fe 500 ton Fe 1984 ~ 30ton-yrs.	$\gtrsim$220 MeV $\pi^{\pm}$ $\gtrsim$190 MeV $\mu^{\pm}$ $\gtrsim$16 MeVγ,$e^{\pm}$	0.3cm thick Fe. 0.5cmx0.5cm flash tubes + Geiger counters. Finest glanularity. Size, 6mx6mx13m.

Table 2-b Water Čerenkov Experiments

I.M.B. 52°N 1570m.w.e.	7000ton H_2O 3300ton H_2O 1982 ~ 1800ton-yrs.	$\gtrsim$380 MeV $\pi^{\pm}$ $\gtrsim$380 MeV $\mu^{\pm}$ $\gtrsim$150 MeVγ,$e^{\pm}$	2048x5"ϕ PMT's covering 1.3% of the surface. 170 photo electrons for $p\rightarrow e^{+}\pi^{\circ}$. ($\mu$-e) 62% detectable.
H.P.W. 1500m.w.e.	780ton H_2O 560ton H_2O 1982 ~ 500ton-yrs.	$\gtrsim$8 MeVγ,$e^{\pm}$	704x5"ϕ PMT's distributed in volume. 600 photo electrons for $p\rightarrow e^{+}$. Proportional wire chamber for anti. Difficulty in pattern recognition.
KAMIOKANDE 26°N 2700m.w.e.	3000ton H_2O 880ton H_2O 1983 ~ 660ton-yrs.	$\gtrsim$200 MeV $\pi^{\pm}$ $\gtrsim$170 MeV $\mu^{\pm}$ $\gtrsim$10 MeVγ,$e^{\pm}$	1000x20"ϕ PMT's covering 20% of the surface. 3560 photo electrons for $p\rightarrow e^{+}\pi^{\circ}$. (μ -e) 70% detectable.

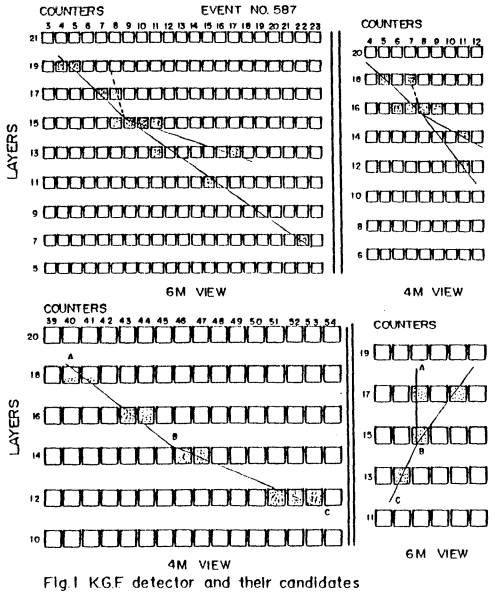

Fig.1 KGF detector and their candidates

either 4m or 6m long. They are proportional counters and hence are capable of measuring the energy loss of the particle in the gas. The two events depicted in Fig. 1 were interpreted by the authors as due to ($p\rightarrow e^{+}\pi^{\circ}$), Event #587, and ($p\rightarrow\mu^{+}K^{\circ}(\pi^{+}\pi^{-})$), Event #877, respectively. Considering, however, the facts that the modular size is 10cm x 10cm

and that the average counter hits are 3~4 per track, it is not easy to exclude the possibility of interpreting them as due to the ν-interactions. One should note also that the derivation of dE/dx from the observed energy loss in a counter depends critically on the path length of the particle in the counter gas which in turn depends strongly on the space reconstruction of the event from the hit counters. There were no Monte-Carlo simulation of ν-interactions in their detector nor accelerator ν-beam test given to the detector. Besides these two events, K.G.F. has a possible candidate of $p \to \bar{\nu} K^+(\mu^+\nu)$, or $p \to \bar{\nu}\pi^+(\pi^+$ scattered).

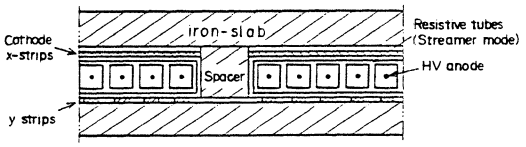

Fig. 2 Detector layer of NUSEX

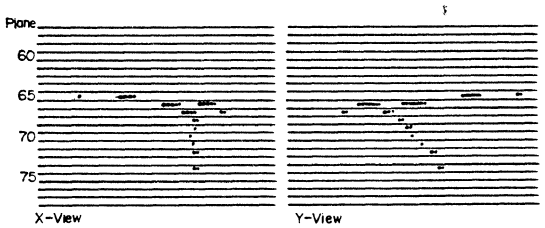

Fig. 3 A candidate of NUSEX

Fig. 2 shows the detector layer of the NUSEX experiment. The same layer of the 1cm x 1cm streamer tube array gives both the X- and the Y-coordinates.

NUSEX observed a candidate for $p \to \mu^+K^\circ(\pi^+\pi^-)$. The event is shown in Fig. 3. It is clear that if it were produced by neutrino the incident direction makes a glancing angle to the Fe plates. It is unfortunate that they did not have the ν-beam test for this incident angle; for, if they did, the ν-background estimation would have been more reliable. NUSEX very recently obtained a possible candidate for $p \to e^+\pi^\circ$.

Fig. 4 shows the Frejus detector which has just entered the game. It features the thin Fe plate of 0.3cm thick and the fine granularity of 0.5cm x 0.5cm flash tubes. It is triggered by the Geiger tube layers. As of July, 1984, it accumulated 30 ton year of exposure and observed 3 contained ν-events. The detector will be 800 tons at the end of 1984 and will be completed to 900 tons in the spring of 1985.

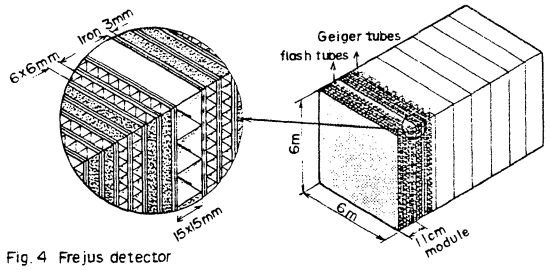

Fig. 4 Frejus detector

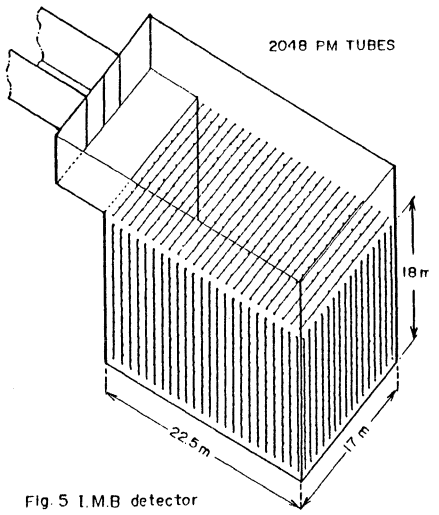

Fig. 5 I.M.B detector

The fact that the early starter K.G.F. reported some candidates claiming the proton decay life time in the range of 10^{30} years created an optimistic atmosphere and it was amplified by the early observation of the above $p \to \mu^+K^\circ$ candidate by NUSEX. This air of optimism was turned into that of pessimism in mid 1983 by the report of the world largest experiment I.M.B.[9], which claimed no candidates for proton decay and set the 90% C.L. lower limit of the partial life time(τ/branching ratio) for $p \to e^+\pi^\circ$ near 10^{32} years.

The experimental lay-out of I.M.B. is shown in Fig. 5. It is essentially a swimming pool dug in the salt mine. It is lined by black plastic sheets and a total of 2048 PMT's of 5" ϕ were installed over the surface. The photocathode coverage amounts to 1.3% of the surface. All the 2048 PMT's are equipped with TDC(1ns x 512) + ADC(9 bits) and the

analysis depends heavily on the timing information. It is estimated that a total of 170 photoelectrons will be observed for $p \to e^+ \pi^\circ$. The back to back two Čerenkov cones of about 80 photoelectrons each would be a very clear and distinct signal for $p \to e^+ \pi^\circ$ in this detector and the fact that they did not observe any such signal put the minimal SU(5) GUT in difficulty. However, as for the other decay modes, like $\mu^+ K^\circ (\pi^+ \pi^-)$, which do not produces well separated prominent $\check{C}$ rings, the detector can not recognize individual $\check{C}$ rings. Their analysis depends on three physical quantities they can measure. They are the E_c (the energy of electro-magnetic shower which produces the observed total number of photoelectrons), the isotropy parameter A (the vector sum of the unit vectors pointed to each hit PMT from the reconstructed origin of the event), and the existence or the non-existence of μ-e decay signal. Since April 1984 the I.M.B. experiment is now reporting the observation of seven possible candidates, each allowing several possible interpretations, of nucleon decay, based on their (E_c - A) analysis.

The experiment H.P.W.[10] is also a water Čerenkov detector but it has a volume distributed PMT array. It certainly has a better light collection efficiency than I.M.B., but on the sacrifice of the event pattern recognition, which is quite serious if one has to fight against a severe ν-background. It is equipped with the anti-counter layer of proportional chamber. They so far reported 2 candidate events with 2 μ-e signals each and a candidate event with 3 μ-e signals. They are; $A_{2\mu}$ of E_c = 600 MeV, A = 0.2, claimed to be consistent with $p \to \mu^+ K^\circ (\pi^+ \pi^-)$, $p \to \mu^+ \rho^\circ (\pi^+ \pi^-)$, and $N \to \mu\mu\nu\pi\cdots$, etc. (Pati-Salam type); $C_{2\mu}$ of E_c = 400 MeV, A = 0.4, claimed to be consistent with $p \to \mu^+ \rho^\circ (\pi^+ \pi^-)$ with π^- absorved, $N \to \mu\mu\nu\pi\cdots\cdots$, etc; and $A_{3\mu}$ of E_c ≒ 840 MeV, A = 0.4, and claimed to be consistent with $N \mu^+ \mu^- \nu \pi \cdots\cdots$. They estimate the 90% upper limit of the ν-background is 0.18 for $A_{2\mu}$ and 0.54 for $C_{2\mu}$. No background estimation is given to $A_{3\mu}$.

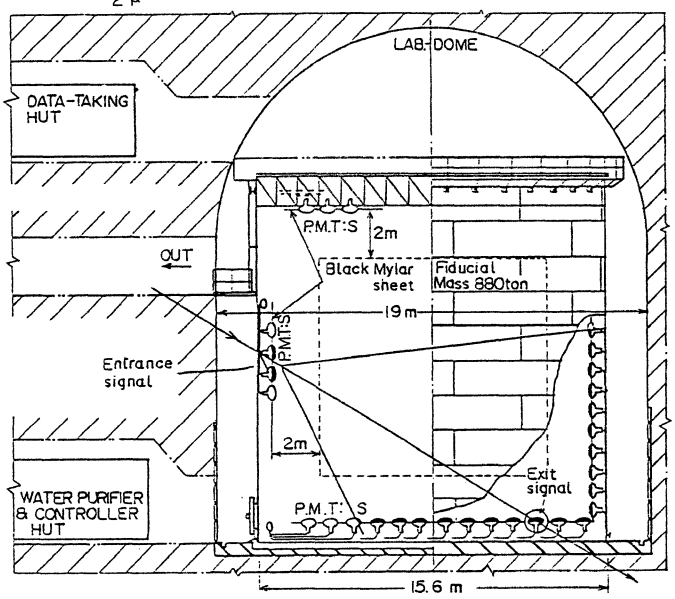

Fig. 6 KAMIOKANDE detector

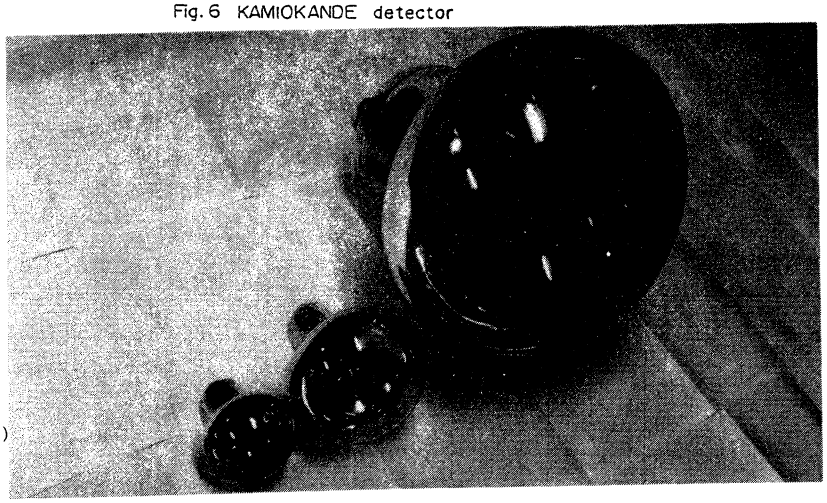

Fig.7
5" (I.M.B.), 8" , and 20" (KAMIOKANDE) PMT's.

The KAMIOKANDE detector is shown in Fig. 6. It is a cylindrical mass of water surrounded by 1000 PMT's 20"ϕ covering 20% of the entire surface. From the very beginning the detector was designed to observe as many possible decay modes as possible of nucleon decay. In order to achieve this goal within a reasonable cost the PMT's of 20" diameter were newly developed specifically for this experiment, see Fig. 7. All the 1000 PMT's are equipped with 15 bits ADC's and $p \to e^+ \pi^0$ is expected to give a total of 3560 photoelectrons. With this light collection efficiency it is possible to clearly recognize all the individual $\check{C}$ rings. The $\check{C}$ rings of stopping particles as observed by I.M.B., Fig. 8-a, and by KAMIOKANDE, Fig. 8-b, are shown for comparison. In Fig. 8-a, the number of prongs indicates the number of photoelectrons observed by each PMT, while in Fig. 8-b the area of the circle is proportional to the photoelectron number observed by each PMT. One can clearly see in Fig. 8-b that the particle scattered twice before it ceases emitting Čerenkov light. Not only that one can observe individual $\check{C}$ rings, down to 10 MeV electron rings, but also the improved light collection allows the separation of showering particles(e , γ) from non-showering particles(μ , π). In the case of a cascade shower a large number of low energy $e^{\pm}$'s are created and they are scattered off the original direction of the primary. Therefore, by observing the radial distribution of photons around the original direction, one can distinguish between the showering and the non-showering cases. The result of such separation is shown in Fig. 9. These two features, the observation of all the individual $\check{C}$ rings and the separation between the showering and the non-showering, are instrumental in reducing the number of possible interpretations of an event as well as in reducing the number of ν-background.

KAMIOKANDE has so far analyzed the data of 660 ton year exposure and obtained 4 possible candidates of nucleon decay above the ν-background at 90% C.L.

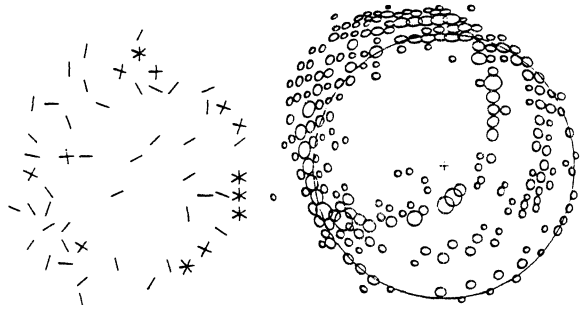

Fig.8-a Stopping particle (IMB)

Fig.8-b Stopping particle (KAMIOKANDE)

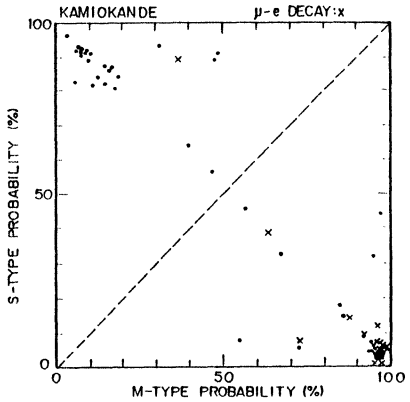

Fig.9 Shower/Non-shower separation

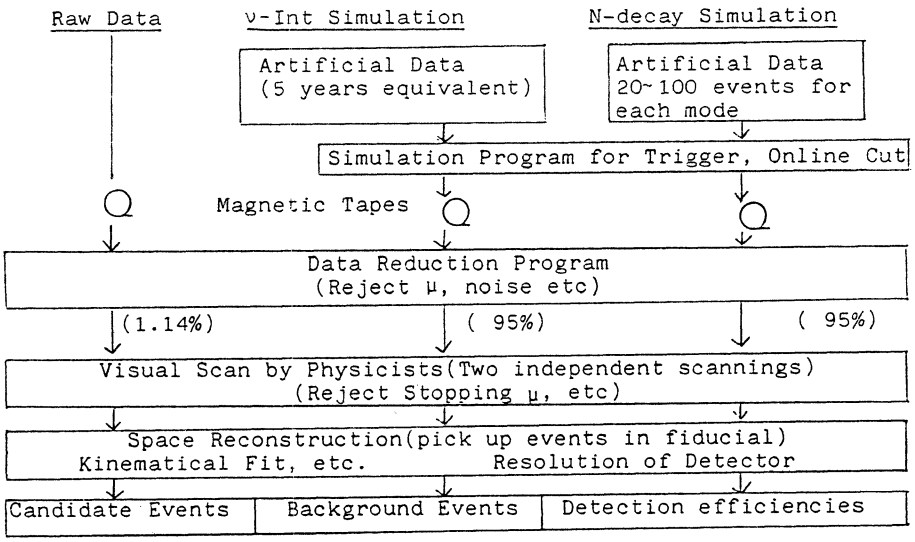

Fig. 10 Data Reduction & Analyses

3. DATA ANALYSES AND ν-BACKGROUND

The data analyses and the estimation of ν-background are similar in I.M.B. and KAMIOKANDE and in what follow we describe those of KAMIOKANDE. In Fig. 10 are shown schematically the procedures.

The raw data are first reduced by computer program in order to eliminate the penetrating μ's, electrical noises etc. The reduced data, 1.14%, are subjected to the visual scanning by two independent groups of physicists. In this visual scan, the stopping μ's, the edge clipping μ's, and the rock showers are easily recognized. The geometrical fitting of $\check{C}$ ring for stopping μ's and/or showers makes a clean distinction between the internally produced μ,e,γ, and those entering from outside the detector when the former is produced at least 1m inside the detecting PMT arrays. The average processing rate is about 15 sec per event and an average of 400 events/day are scanned. The fully contained events thus obtained are subjected to the full analyses; i.e. the space reconstruction, the shower/non shower discrimination, and the invariant masses. The analyses at this stage is like those of analysing the pictures of bubble chamber. Namely, one assign particle species to each of the observed prongs and see the overall fit of the event. Therefore, the observation of all the individual $\check{C}$ rings and the separation of shower/non shower play the essential role in reducing the number of possible interpretations.

The ν-interactions expected for 5 year exposure are Monte Carlo simulated by using the existing data of ν-experiments and the flux of atmospheric neutrinos as estimated by T.Gaisser et al[11]. Using the observed quasi elastic charged current events, the estimated ν flux was found to be good to better than 20%. The simulated events were subjected to the same analysis program as the real data in order to estimate the number of ν-background for various decay modes.

Various modes of nucleon decay have also been simulated by Monte Carlo method and the generated events, 20~100 in number for each decay mode, were subjected to the same analysis program as the real data in order to estimate the detection efficiencies of various decay modes.

It should be noted that the ν-interactions and/or the nucleon decays occuring in the nucleus get distorted substantially by the secondary nuclear effects; i.e., the produced mesons, π,K, ρ etc., get absorbed, scattered, and charge-exchanged. Our present knowledge of these nuclear effects is expected to be good enough for predicting the average behavior. However, it is not the average behaved ν-interactions in nucleus which mimic the nucleon decay and it is in the tail of the distribution where this mimicking occurs. In this sense, a better understanding of the nuclear effects is strongly desired. The best way is to make the ν-beam test for a scaled-down detector.

The NUSEX experiment did have such ν-beam test for a part of their detector but, as mentioned before, the test was not quite sufficient for such anisotropic detector.

The experiments of H.P.W. and K.G.F. have neither the detailed Monte Carlo simulation nor the ν-beam test. The estimation of ν-background and detection efficiency in these experiments should be taken with due reserve.

4. RESULTS AND DISCUSSION

The great majority of the observed contained events can be explained in terms of the atmospheric ν's.

Fig. 11 shows the number of contained events versus the exposure, Kiloton year, for the on-going experiments. They are consistent within 20% with the expectation of the atmospheric neutrinos when the difference in detection thresholds is taken into account. The energy spectrum and the rate of the pseudo-elastic charged current events are also in reasonable agreement with the expectation as shown in Fig. 12-a and Fig. 12-b. The prong-multiplicity distribution is also in reasonable agreement with the expectation as shown in Fig. 13.

The number of possible candidates is plotted in Fig. 14 against the exposure. Here

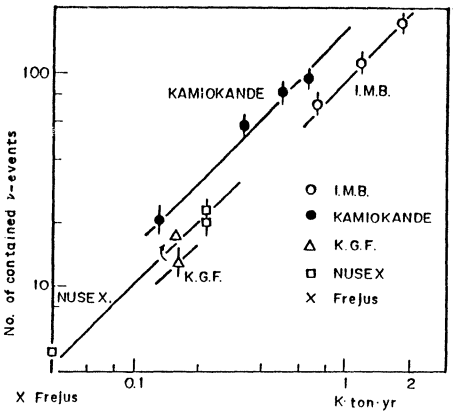

Fig. 11 Observed contained event

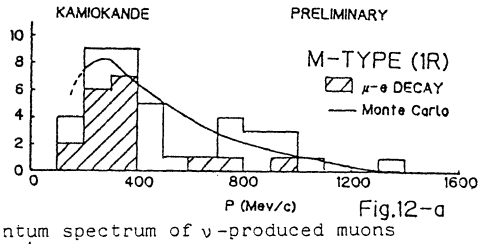

Fig.12-a

Momentum spectrum of ν-produced muons

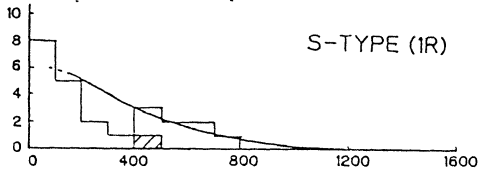

Momentum spectrum of ν-produced electrons

Fig.12-b

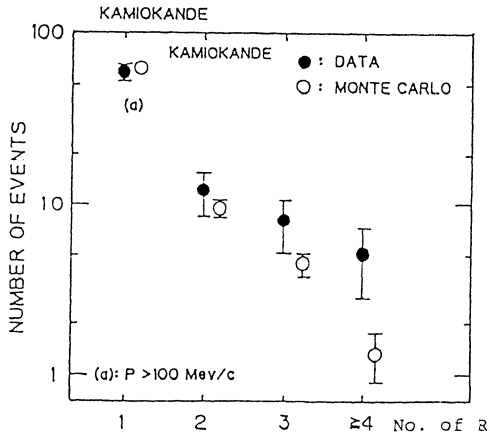

Fig.13 Multiplicity distribution

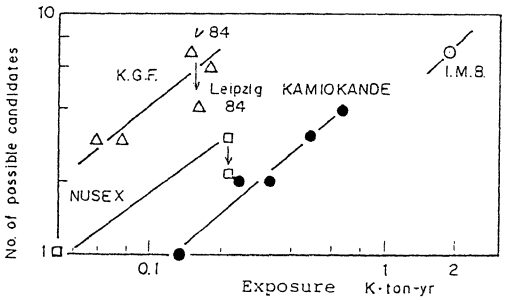

Fig. 14 Number of possible candidates versus exposure

we notice some difference among the various experiments in the level of acceptance as the possible candidates. The 90% C.L. lower limits for τ/B, background unsubtracted, as given by these experiments are summarized in Fig. 15. In the figure the number of the pips attached to the symbols indicates the number of possible candidates claimed by the experiment. The results of KAMKOKANDE are shown separately in Table 3 in which the detection efficiency, the estimated ν-background together with its 90% C.L. upper limit, and the number of candidates are also given for each investigated decay channels.

One notices that in some decay channels the number of possible candidates exceeds the 90% C.L. upper limit of ν-background.

The situation is visually summarized in Fig. 16-a and Fig. 16-b. In Fig. 16-a the number of possible candidates is plotted against the estimated ν-background for the decay modes of (N → charged anti-lepton + X) satisfying $\Delta B = \Delta L$. Fig. 16-b shows the same plot for the decay modes of (N→anti-neutrino + X) satisfying $\Delta B = \Delta L$.

It thus seems that we are observing some signals above, at 90% C.L., the ν-background and that those events are consistent with some of the decay modes of nulceon decay.

It is, however, still premature to conclude that protons do decay, for the issue is of the gravest significance to the future of elementary particle physics. We have to accumulate more data to improve the satistical significance and also we have to improve our understanding of ν-interactions in nuclei in order to fight successfully against the small signal noise ratio of 1/20 or less.

The four candidate events of KAMIOKANDE are shown in Figs. 17-a, -b, Fig. 18-a, -b, Fig. 19-a, -b, and Fig. 20-a, -b. In Figs. -a are shown the events in the exploded view in which the tin-can configuration of the PMT array is cut at side, top and bottom open, and the size of the circle indicates the pulse height of the individual PMT. At lower right of the figure the record of the transient digitizer covering 10μ sec period is shown. One sees the μ-e decay signal in some of the events. In Figs. -b the same events

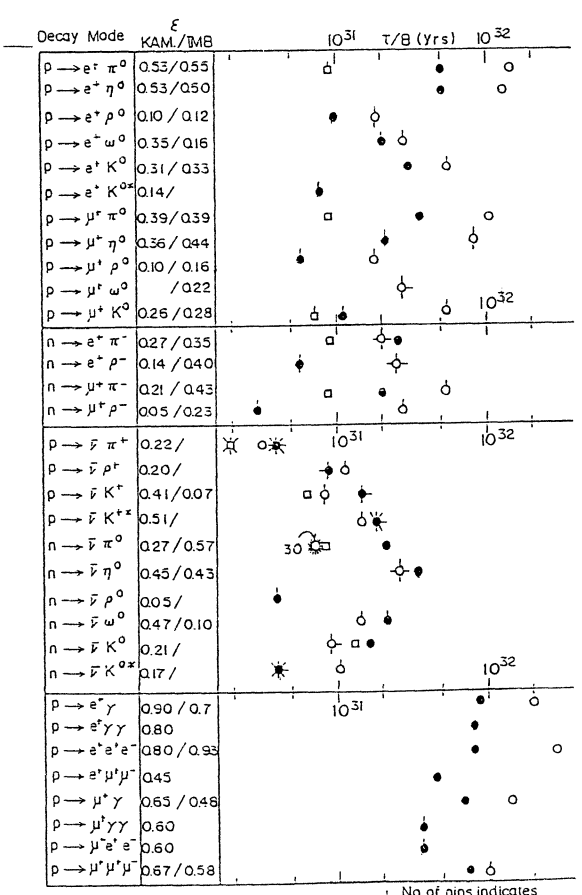

Fig. 15 The 90% C.L. lower limits of τ/B in years

Table 3 90% C.L. lower limits of τ/B(KAMIOKANDE)

Decay Mode	Detection Efficiency	ν-B.G.(upper limit 90%C.L.)	Number of Candidates	Lower limit 90% C.L. τ/B in 10^{31}yrs.
$p \to e^+ \pi^0$	0.53	0	0	5.1
$p \to e^+ \eta^0$	0.53	0	0	5.1
$p \to e^+ \omega^0$	0.35	0.3/(0.8)	1	2.0
$p \to e^+ \rho^0$	0.10	0.5	0	1.0
$p \to e^+ K^0$	0.31	0	0	3.0
$p \to e^+ K^{*0}$	0.14	0.3/(0.8)	1	0.8
$p \to \mu^+ \pi^0$	0.39	0.2	0	3.8
$p \to \mu^+ \eta^0$	0.36	0/(0.3)	1	2.1
$p \to \mu^+ \rho^0$	0.10	0.2/(0.6)	1	0.6
$p \to \mu^+ K^0$	0.26	0.2/(0.6)	2	1.1
$n \to e^+ \pi^-$	0.27	0.2	0	2.6
$n \to e^+ \rho^-$	0.14	0.3/(0.8)	2	0.6
$n \to \mu^+ \pi^-$	0.21	0	0	2.0
$n \to \mu^+ \rho^-$	0.05	0.3/(0.8)	1	0.3
$p \to \bar{\nu} \pi^+$	0.22	13.5	8	0.4
$p \to \bar{\nu} \rho^+$	0.20	1.8/(2.7)	3	0.9
$p \to \bar{\nu} K^+$	0.41	2.1/(3.0)	3	1.5
$p \to \bar{\nu} K^{*+}$	0.51	3.8/(4.9)	6	1.7
$n \to \bar{\nu} \pi^0$	0.27	1.3	0	2.1
$n \to \bar{\nu} \eta^0$	0.35	0	0	3.4
$n \to \bar{\nu} \omega^0$	0.47	1.3	1	2.1
$n \to \bar{\nu} \rho^0$	0.05	1.5	1	0.4
$n \to \bar{\nu} K^0$	0.21	0.5	0	1.6
$n \to \bar{\nu} K^{*0}$	0.17	3.8/(4.9)	7	0.4
$p \to e^+ \gamma$	0.90	0	0	8.7
$p \to e^+ \gamma\gamma$	0.80	0	0	7.7
$p \to e^+ e^+ e^-$	0.80	0	0	7.7
$p \to e^+ \mu^+ \mu^-$	0.45	0	0	4.3
$p \to \mu^+ \gamma$	0.65	0	0	6.2
$p \to \mu^+ \gamma\gamma$	0.53	0/(0.3)	1	3.0
$p \to \mu^+ e^+ e^-$	0.53	0/(0.3)	1	3.0
$p \to \mu^+ \mu^+ \mu^-$	0.67	0	0	6.4
$n \to \bar{\nu} \mu^+ \mu^-$	0.33	0.3	0	3.2
$n \to \bar{\nu} e^+ e^-$	0.71	0.8/(1.4)	3	2.4
$n \to \bar{\nu} \gamma$	0.31	6.0	4	2.2
$n \to \bar{\nu} \gamma\gamma$	0.71	0.3/(1.4)	3	2.4

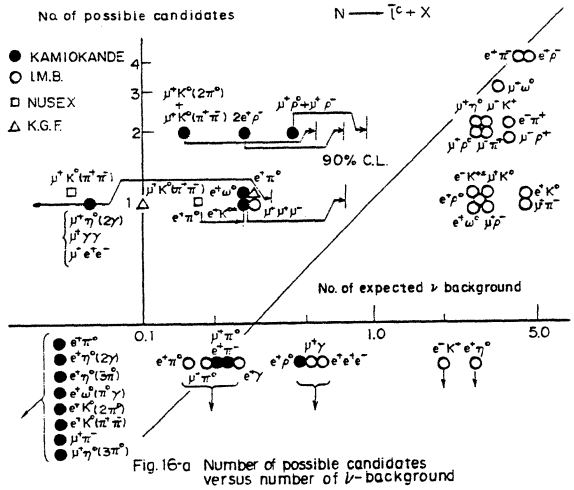

Fig. 16-a Number of possible candidates versus number of ν-background

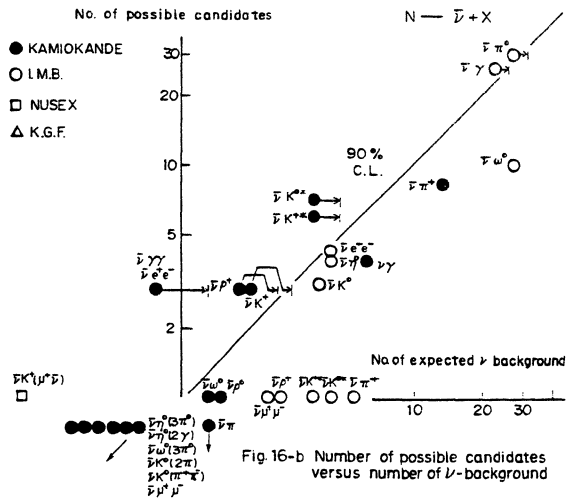

Fig. 16-b Number of possible candidates versus number of ν-background

are shown, respectively, in the spherical view in which the light attenuation in water as well as the directional dependence of PMT sensitivity is corrected for. The left hand figure shows the forward hemisphere as seen from the event vertex. The circle at about half the radius indicates the 41.6° cone corresponding to the β = 1 particle, while the inner circle is for the muon of the velocity corresponding to the number of photo-electrons in the ring. The right hand figure shows the backward hemisphere.

We now look at these events individually. For each Čerenkov ring the number of photoelectrons was counted in the 45° cone and at this stage one should allow 15% error for the energy and/or the momentum assigned to each ring. S or M denotes whether it is showering type, e, γ, π^0 or meson type, μ, π (non-showering).

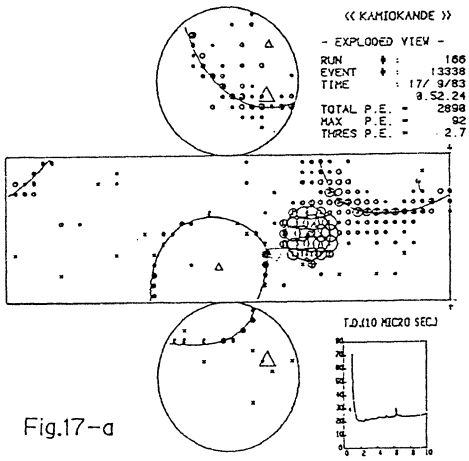

Fig.17-a

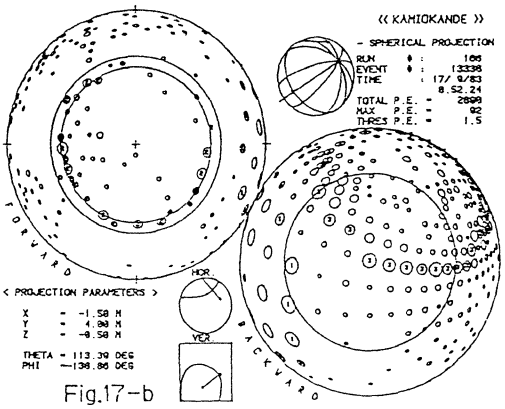

Fig.17-b

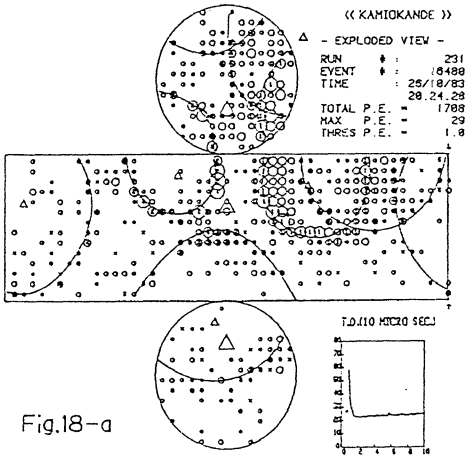

Fig.18-a

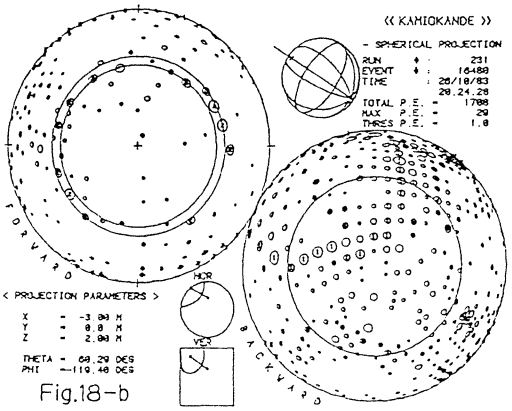

Fig.18-b

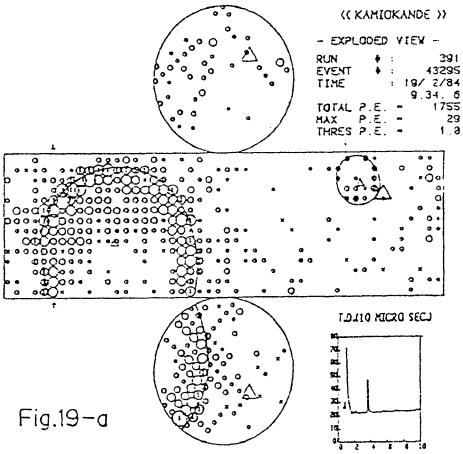

Fig.19-a

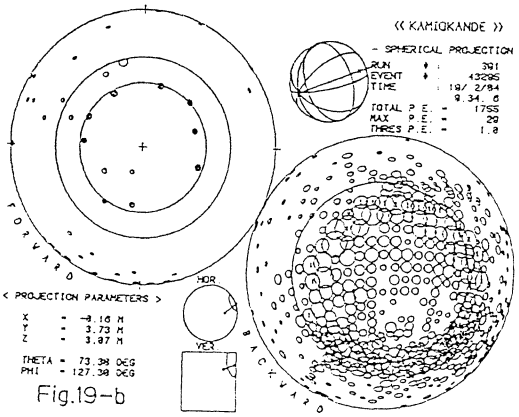

Fig.19-b

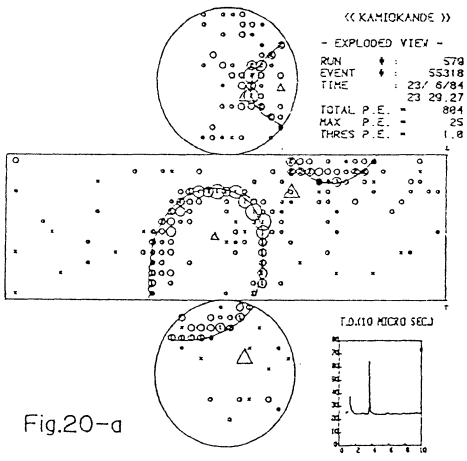

Fig.20-a

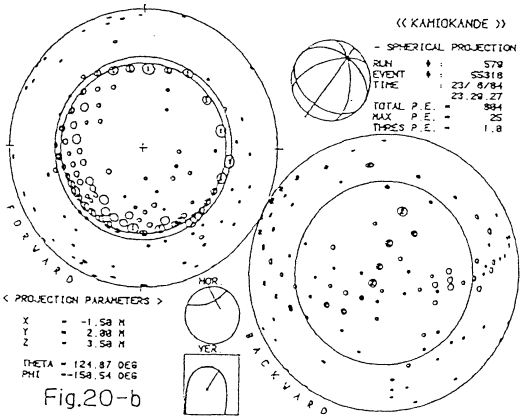

Fig.20-b

1. Event #166-13338; Total photoelectron number 2890, μ-e Yes/No

Ring #1,1202 photoelectrons, S/M,462 MeV/c (e,γ),595 MeV/c (μ), 800 MeV/c (π).

Ring #2, 184 photoelectrons, M, 367 MeV/c (π), 249 MeV/c (μ).

Ring #3, 819 photoelectrons, S, 320 MeV/c (e,γ).

$\theta_{12} = 101^\circ$, $\theta_{23} = 133^\circ$, $\theta_{31} = 106^\circ$, and $\theta_{12} + \theta_{23} + \theta_{31} = 340^\circ$.

$M_{1,2}(\pi^\circ,\pi) = 670$ MeV, $M_{3,1,2}(e,\pi^\circ,\pi) = 1100$ MeV and P =380 MeV/c.

Possible interpretation; $n \rightarrow e^+\rho^-(\pi^\circ\pi^-)$.

$M_{1,3}(e\gamma\pi^\circ, e\gamma\pi^\circ) = 610$ MeV, $M_{2,1,3}(\mu, e\gamma\pi^\circ, e\gamma\pi^\circ) = 980$ MeV and P = 380 MeV/c.

Possible interpretations; $p \rightarrow \mu^+\eta^\circ(2\gamma)$, $\mu^+\gamma\gamma$, $\mu^+e^-e^+$, $\mu^+K^\circ(2\pi)$.

2. Event #231-16480; Total photoelectron number 1708,μ-e No.

Ring #1, 548 photoelectrons, S likely, 216 MeV/c (e,γ).

Ring #2, 366 photoelectrons, S/M, 118 MeV/c(e,γ),402 MeV/c(π).

Ring #3, 192 photoelectrons, S/M, 80 MeV/c(e,γ),357 MeV/c(γ).

Ring #4, 201 photoelectrons, S likely, 83 MeV/c (e,γ).

Ring #5, 266 photoelectrons, S likely, 109 MeV/c (e,γ).

$M_{3,4}(\gamma,\gamma) = 130$ MeV, $M_{2,3,4,5}(\pi,\gamma,\gamma,\gamma) = 620$ MeV, $M_{1,2,3,4,5}(e,\pi,\gamma,\gamma,\gamma) = 880$ MeV,
P = 250 MeV/c.

Possible interpretation; $p \rightarrow e^+\omega^\circ(\pi^+\pi^\circ\pi^-)$,

$M_{1,5}(\gamma,\gamma) = 110$ MeV, $M_{2,1,5}(\pi,\gamma,\gamma) = 680$ MeV, $M_{1,2,3,4,5}(\gamma,\pi,\gamma,e,\gamma) = 880$ MeV, P = 250 MeV/c.

Possible interpretation; $n \rightarrow e^+\rho^-(\pi^-\pi^\circ)$.

$M_{1,5}(\gamma,\gamma) = 110$ MeV, $M_{1,2,3,5}(\gamma,\pi,\gamma,\gamma) = 780$ MeV, $M_{1,2,3,4,5}(\gamma,\pi,\gamma,e,\gamma) = 880$ MeV,
P = 250 MeV/c.

Possible interpretation; $p \rightarrow e^+K^{\circ *}(\pi^+\pi^\circ\pi^-)$.

$M_{1,2,3,4,5}(\gamma,\pi,\gamma,\gamma,\gamma) = 880$ MeV, Assume $1\bar{\nu}$ with $p(\bar{\nu}) = 50$ MeV/c,then $M_{total} = 940$ MeV,
P = 200 MeV/c.

Possible interpretations;$p \rightarrow \bar{\nu}\rho^+(\pi^\circ\pi^+)$, $n \rightarrow \bar{\nu}K^{\circ *}(\pi^+\pi^\circ\pi^-)$, and $p \rightarrow \bar{\nu}K^{+ *}(\pi^+\pi^\circ\pi^-)$.

3. Event #391-43295; Total photoelectron number 1755,μ-e Yes.

Ring #1 1406 photoelectrons, S, 535 MeV/c(e,γ, π°).

Ring #2, 43 photoelectrons, M, 219 MeV/c(π), 175 MeV/c(μ).

$\theta_{12} = 166^\circ$, $M_{12}(\pi^\circ,\pi) = 720$ MeV, P = 320 MeV/c. Assume $1\mu^+$ with $p(\mu^+) = 130$ MeV/c
then $M_{total} = 940$ MeV, P = 200 MeV/c.

Possible interpretation; $n \rightarrow \mu^+\rho^-(\pi^\circ\pi^-)$.

Assign π°, μ to rings 1,2 and assume $1\ \pi^+$ with $p(\pi^+) = 170$ MeV/c then $M_{total} = 940$ MeV,
P = 200 MeV/c.

Possible interpretation; $n \rightarrow \mu^+\rho^-(\pi^\circ\pi^-)$.

Assign π°,π to rings 1,2 and assume $1\bar{\nu}$ with $p(\bar{\nu}) = 160$ MeV/c, then $M_{total} = 940$ MeV,
P = 170 MeV/c.

Possible interpretation; $p \rightarrow \bar{\nu}\rho^+(\pi\ \pi^+)$.

4. Event #579-55318; Total photoelectron number 804, μ-e Yes.

Ring #1, 404 photoelectrons, M, 337 MeV/c(μ), 477 MeV/c(π).

Ring #2, 203 photoelectrons, M, 253 MeV/c(μ), 374 MeV/c(π).

$\theta_{12} = 146^\circ$, $M_{1,2}(\pi,\pi) = 850$ MeV and P = 290 MeV/c.

Assume $1\ \mu^+$ with $p(\mu^+) = 0$ MeV/c, then $M_{total} = 960$ MeV,P = 290 MeV/c.

Possible interpretation; $p \rightarrow \mu^+\rho^\circ(\pi^+\pi^-)$.

Assume $1\bar{\nu}$ with $p(\bar{\nu}) = 70$ MeV/c, then $M_{total} = 940$ MeV,P = 220 MeV/c.

Possible interpretation; $n \rightarrow \bar{\nu}\rho(\pi^+\ \pi^-)$.

Assign μ, π(π, μ) to rings 1,2 and assume 1π with $p(\pi) = 130$ MeV/c(130 MeV/c), then M_{total} = 940 MeV, P=100 MeV/c(190 MeV/c).

Possible interpretation; $p \rightarrow \mu^+K^\circ(\pi^+\pi^-)$.

There is another physical process of great interest related to proton decay. It is the catalysis of nucleon decay by the magnetic monopole. GUTS in general predict the presence of magnetic monopole of mass around 10^{16} GeV. If the magnetic monopole was indeed created at the time of Big Bang and if it indeed catalyses the nucleon decay, we can expect to see a series of two or more nucleon decay events in a large proton decay detector. Serious searches were made for such processes in I.M.B. and in KAMIOKANDE.

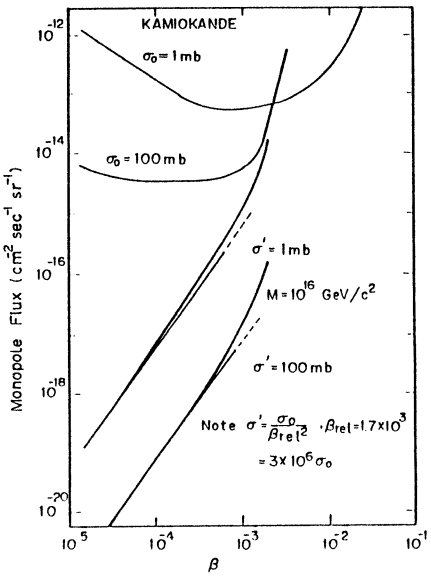

Fig. 21 The 90% C.L. upper limits of Magnetic monopole

Table 4 Expected Low Energy Neutrino Events

Source of ν	Solar B^8	Solar Bubakov effect	Gravitational collapse at Galactic Center
E ν_e	$E\nu_e \leq 14$ MeV $<E\nu_e>\sim 10$ MeV	$E\nu_e \leq 53$ MeV $<E\nu_e>\sim 35$ MeV	$<E\nu_e>\sim 16$ MeV
$^{12,13,14}\nu_e$ flux at Earth	5.6×10^6 ν_e /cm^2/sec.	1.2×10^4 ν_e /cm^2/sec.	$7.7\times10^{10}\nu_e$/m.sec cm^2 for a few m.sec. duration
KAMIOKANDE 880 ton H_2O	6.0($\nu_e e \to \nu_e e$) per day. ($E_e \geq 6$ MeV)	35 $\nu_e e \to \nu_e e$ 53 $\nu_e O \to e^- F$ per year. ($E_e \geq 6$ MeV)	2.3($\nu_e e \to \nu_e e$) per m.sec.burst ($E_e \geq 6$ MeV)
JACK 22000 ton H_2O	150($\nu_e e \to \nu_e e$) per day. ($E_e \geq 6$ MeV)	2.4($\nu_e e \to \nu_e e$) 3.6($\nu_e O \to e^- F$) per day. ($E_e > 6$ MeV)	58($\nu_e e \to \nu_e e$) per m.sec.burst ($E_e \geq 6$ MeV)
	$\bar{\theta}_{\nu_e - e} \leq 19°$.	$\bar{\theta}_{\nu_e - e} \leq 10°$.	$\bar{\theta}_{\nu_e - e} \leq 14°$.
	$\bar{\theta}$ (8→4 MeV) scatt = 100°.	$\bar{\theta}$ (16→8 MeV) scatt = 50°.	$\bar{\theta}$ (12→6 MeV) scatt = 65°.
	Source direction $\leq 8°$ per day.	Source direction $\leq 6°$ per month.	Source direction $\leq 2°$ per m.sec.burst

The results of KAMIOKANDE are given in Fig. 21 in the form of 90% C.L. upper limit of the flux of magnetic monopole for two assumed values of catalysis cross-section.

If the low velocity magnetic monopoles were trapped in the Sun, we can expect some flux of $\pi^+ \to \mu^+ \to e^+$ decay neutrinos from the Sun resulting from the catalysed nucleon decay. Search was made to look for the neutrino produced electrons of ~ 35 MeV in the fiducial volume. The results are also shown in Fig. 21, lower two curves.

5. FUTURE PROSPECTS

There are a number of future projects of nucleon decay experiment, some under construction and some in planning stage.

They are;

I.M.B. Improvement in photon detection efficiency.(Funded)

Additional 2048 x 8" ϕ PMT's plus waveshifter plates to cover eventually 9% of the surface.

K.G.F. A new 300 ton detector at 2000 m.level.(Funded)

6x6x6.5m^3. Thin Fe plates + 4000 prop.counters. A proposal to build 500ton calorimeter at 2000m depth in '85 to '86.

H.P.W. A proposal(by end of '84) to build large liq. Ar drift chamber. Aims: High resolution search of N-decay and Solar B^8 ν's.

SUDAN II (Minnesota-Argonne-Oxford-Ratherford-Tufts)(Funded)

1200 ton fine grain calorimeter of honeycomb structure with dE/dx capability. Under construction. Expected data taking early 1987. Fe 2.4mm thick.

KAMIOKANDE II Install 4π anti counter layers and timing circuit by end 1984.(Funded). Data taking early '85. Solar $B^8\nu$'s will be looked for. In collaboration with American physicists.

Super-KAMIOKANDE(or JACK) A proposal in mid'85 to build 40mϕ x 40mh water $\check{C}$,(32 Kton total, 22 Kton fiducial containing 2.5 Kton free proton) with 40% surface coverage by PMT (~11000)of 20" ϕ . Complete anti-coincidence and(timing + amplitude) for all PMT. Aims: High resolution study of N-decays, Solar B^8 ν's, and ν's from possible gravitational

collapse of star in Milky Way.

As an example, the Super-KAMIOKANDE(or JACK) is shown in Fig.22. It will not only collect the events at 25 times the rate of KAMIOKANDE, including those of 2.5 Kton free proton, but also promisses to obtain the signals of celestial neutrinos as shown in Table. 4.

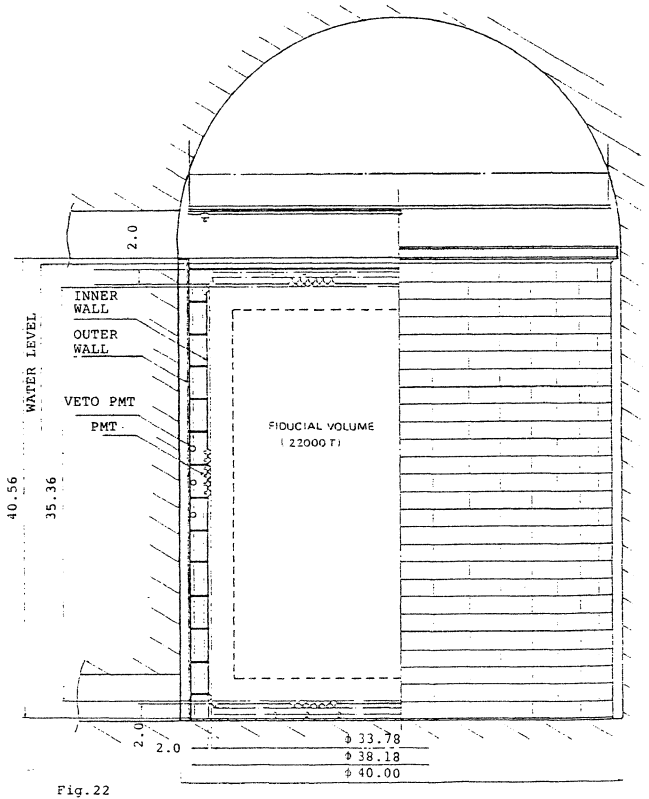

Fig.22
Super-KAMIOKANDE(or JACK)

6. CONCLUSIONS

We may now conclude that:

(1) The great majority of the observed contained events in the on-going experiments are due to the atmospheric neutrinos of Cosmic Ray origin.

(2) However, there are a number of events defying the above explanation at 90% C.L. The rate is about 5% of the neutrino events and these events are consistent with some of the nucleon decay modes. What are they? The answer has to await more data of still better resolution together with an improved understanding of the nuclear effects. For the former a number of next generation experiments are getting ready and for the latter the ν-beam test of the detector is strongly desired.

(3) Water can be made into a very precise particle detector when provided with a sufficient photocathode coverage, $\gtrsim 20\%$, of the whole surface. It also gives the hope of observing Solar B^8 ν's by means of the elastic ν_e-e scattering in which the scattered electrons reflect the direction and the energy spectrum of the incident neutrinos.

(4) The Rubakov effect of the magnetic monopoles has not been observed and the flux upper limits are given.

In conclusion, the author acknowledges with gratitude the support by the Ministry of Education, Japan. The expert help of Dr.Spiering, scientific secretary, is also appreciated.

REFERENCES

(1) The Present Status of Grand Unification and Proton Decay; P.Langacker, University of Pennsilvania Preprint, UPR-0263T, June 28, 1984.

(2) Proton Decay Experiments; D.H.Perkins, CERN Preprint,CERN/EP 84-7, January 26, 1984. To appear in Annual Reviews.

(3) J.C.Pati and A.Salam; Phys.Rev.Lett.31, 661(1973) and Phys.Rev.D8, 1240(1973).
(4) H.Georgi and S.L.Glashow; Phys.Rev.Lett.32,438(1974).
(5) KAMIOKANDE(KAMIOKA Nucleon Decay Experiment); Tokyo-KEK-Niigata collaboration.
K.Arisaka et al.; LICEPP preprint U. of Tokyo(UTLICEPP 82-04), 1982.
M.Koshiba; ICOBAN '84, Park City, Utah.
Y.Totsuka; XIXth Moriond Conf. 1984.
M.Koshiba; XXII Inf. Conf. on High Energy Physics, Leipzig, 1984.
(6) Frejus experiment; Aachen-Orsay-Palaiseau-Saclay-Wuppertal collaboration.
R.Barloutaud, et al.; Proc. Int. Coll. Baryon Non-Conservation, Bombay, 1982, P143.
R.Barloutaud,; ICOBAN, Park City, Utah '84.
S.Julian; XXII Int. Conf. on High Energy Physics, Leipzig, 1984.
(7) NUSEX experiment; CERN-Frascati-Milano-Torino collaboration.
G.Battistoni, et al.; Phys. Lett. 118B,461(1982).
G.Battistoni, et al.; Phys. Lett. 133B,454(1983).
G.Battistoni and E.Iarocci; ICOBAN '84, Park city, Utah, 1984.
S.Ragazzi; XIXth Moriond Conf., 1984.
E.Fiorini; XXII Int. Conf. on High Energy Physics, Leipzig, 1984.
(8) K.G.F. experiment; Tata-Osaka City-Tokyo collaboration.
M.R.Krishnaswamy, et al.; Phys. Lett., 106B,339(1981).
M.R.Krishnaswamy, et al.; Phys. Lett., 115B,349(1982).
V.S.Narasimham; ICOBAN '84, Park City, Utah, 1984.
V.S.Narasimham; XXII Int. Conf. on High Energy Physics, Leipzig, 1984.
(9) I.M.B. experiment; Irvine-Michigan-Brookhaven collaboration.
R.M.Bionta et al.; Phys. Rev. Lett. 51,27(1983).
B.G.Cortez et al.; Phys. Rev. Lett. 52,1092(1984).
G.W.Foster and W.Gajewski; ICOBAN '84, Park City, 1984.
E.Shumard; XIXth Moriond Conf., 1984.
J.LoSecco; XXII Int. Conf. on High Energy Physics, Leipzig,1984. In preparing Fig.15, the I.M.B. detector efficiency, , was calculated by taking the average of the four different estimates supplied by Dr.J.LoSecco. He also sent the author the latest reanalysis,(provisional), of the events of I.M.B., but time did not allow the alteration of this text.
(10) H.P.W. experiment; Harvard-Purdue-Wisconsin collaboration.
J.A.Gaidos et al; Proc. 1982 Summer Workshop on Proton Decay Exp., ANL, 1982, P131.
R.Loveless; ICOBAN '84, Park City, 1984.
D.Cline; XXII Int. Conf. on High Energy Physics, Leipzig, 1984.
(11) T.K.Gaisser et al.; Proc. Fourth Workshop on Grand Unification, Pennsylvania(1983)..
T.K.Gaisser et al.;"The flux of atmospheric neutrinos",BA-83-20.
T.K.Gaisser et al.; Phys. Ref. Lett. 51,223(1983).
Neutrino flux at KAMIOKA; private communication with T.K.Gaisser.
(12) J.N.Bahcall et al.; Rev. Mod. Phys., 54 767(1982).
(13) J.Arafune et al.; P.R.L., 50, 1901(1983) and P.L.B.(1983).
(14) T.J.Mazurek et al.; DUMAND, Hawaii(1980).

LoSecco,J; I.M.B. has not yet made use of much of the information in their events. We can use information about # tracks, energies and angles to reduce the background and to constrain the events.
Koshiba,M; It would be nice if you can do that.
Fiorini,E; I would like to make a few statements regarding the results of NUSEX collaboration.
1. We never claimed to have discovered nucleon decay. We only presented two candidates, where the background of neutrino interactions is low. I understand it can be dangerous to indicate $\pi^{\circ}e^{+}$ decay, after the negative result of I.M.B. and KAMIOKANDE, and the consequent impopularity in theory. However we cannot(and do not want) hide this candidate below the carpet: We can only state that neutrino background is < 0.28 at 90%

C.L.

2. We are the only collaboration which present the candidates without any line, ring, circle added. We present only the output of the computer without any make-up. Maybe we are conservative, but we like this way.

3. We exposed a part of our detector not only to neutrinos, but also to pions, muons and electrons, and we were the only ones to do so. Our background was obtained from real electron and neutrino events. I agree with you that our test on neutrino was limited, but I believe that you agree with me that a limited experimental test is better than no test at all.

4. For some of the decay channels, NUSEX has a sensitivity similar to I.M.B. and KAMIOKANDE, and I would like you to present our limits on nucleon decay too.

Koshiba,M; Your lifetime point was put in the diagram.

Ioffe; I wish to ask the speaker to pay attention that these exist a reliable calculation of matrix element of proton transitions into quark current, based on the QCD sum rule appoach and done in a modelless way. This calculation gives a rather good accuracy predictions for branching ratio of $e^+\pi^o$ is about 50%. The proton life-time was also found with rather good accuracy up to the over whole uncertainty in ΛQCD. With account of this uncertainty the upper limit for proton life-time is $4 \cdot 10^{30}$ years.

Koshiba,M; Thank you.

Jarlskog,C; What is the present limit on the neutron-antineutron oscillation time?

Koshiba,M; I did not think it was ripe to be included in this talk.

LoSecco,J; $\tau(n \to \bar{n}) > 9 \times 10^7$ sec from I.M.B. Using Doven et al. calculation to convert from bound to free lifetime. This limit includes 5 events background(or candidates).